Journal of
Engineering Sciences
Faculty of Engineering
Assiut University
JES
مجلة
العلوم الهندسية
كلية الهندسة
جامعة أسيوط
journal homepage: http://jesaun.journals.ekb.eg

Numerical Investigation on the Effect of the Azimuthal Deviation on the Performance of Equal Speed Co-Rotating Double Rotor Small-Scale Horizontal-Axis Wind Turbine

Received 27 September 2023; Revised 20 November 2023; Accepted 20 November 2023

A. Abdelfattah [1]
M.F. EL-Dosoky [2]
O. Hassan [3]
M.M.S. Ahmed [4]
Ahmed Hamza H. Ali [5]

Keywords
Wind Turbine;
Small Horizontal Axis Wind Turbine;
Double Rotor;
Tip Speed Ratio;
Power Coefficient;
Thrust Coefficient.

Abstract

A double-rotor setup is a promising approach to increase wind turbine power extraction. One common double-rotor configuration is the co-rotating-equal-speed arrangement. The performance of this setup is affected by the azimuthal deviation between the two rotors, which remains constant during rotation. To identify the impact of azimuthal deviation, a numerical investigation was conducted using 10 m/s input wind speed and 0.9 m turbine diameter. The separation distance between the two rotors varied for two values of 0.14 and 0.25 rotor-diameter. The power coefficient of both rotors and the overall turbine were analyzed at different azimuthal deviations using Reynolds-averaged Navier–Stokes $k-\omega$ SST equations. The azimuthal deviation was positive when the front rotor preceded the rear and negative when the rear preceded the front. At 0.14 rotor-diameter separation, positive deviation increased the front rotor power coefficient but decreased the rear's, while negative deviation had the opposite effect on both rotors. The maximum changes in the power coefficient of the front and rear rotors at tip speed ratio of 5 were $\Delta C_P = 0.058$ and $\Delta C_P = 0.066$, respectively. However, the net harvesting power by the double-rotor wind turbine exhibited slight marginal change of $\Delta C_P = 0.008$ at a tip speed ratio of 5. In contrast, at the greater separation, the power coefficients of both rotors and the overall turbine showed slight change with the variation of the azimuthal deviation with a marginal change of $\Delta C_P = 0.012$ at a tip speed ratio of 5. Moreover, the highest increase in the power coefficient was 15% compared to single rotor.

[1] Department of Mechanical Engineering, Assiut University, Assiut, Egypt
[2] Department of Mechanical Engineering, Assiut University, College of Engineering, Fahad Bin Sultan University
[3] Department of Mechanical Engineering, Assiut University, Assiut, Egypt
[4] Department of Mechanical Engineering, Assiut University, Assiut, Egypt
[5] Department of Mechanical Engineering, Assiut University, Assiut, Egypt

https://doi.org/10.21608/jesaun.2023.239362.1267

Nomenclature:

C	Chord length (m).
C_P	Power Coefficient = $\Omega T/0.5\rho AV_\infty^3$.
C_{ps}	Static pressure Coefficient = $(p-p_\infty)/0.5\rho V_\infty^2$.
C_F	Axial thrust coefficient = $F_a/0.5\rho AV_\infty^2$
D_f	Front rotor diameter (m).
D_r	Rear rotor diameter (m).
DR	Diameter ratio = D_f/D_r.
F_a	Axial thrust (N)
k	Turbulence kinetic energy (m^2/s^2).
p	Pressure (Pa).
R	Rotor radius (m).
r	Radial distance (m).
SR	Rotor spacing Ratio = X/D_f.
T	Torque (N.m).
TSR	Tip speed ratio = $\Omega R/V_\infty$.
U	Blade tangential velocity = Ωr
V	Absolute velocity magnitude (m/s).
V_∞	Free stream velocity magnitude (m/s).
W	Relative velocity (m/s).
	Greek letters:
α	Angle of attack (degree).
β	Relative flow angle (degree).
θ	Pitch angle (degree).
ε	Turbulent dissipation rate (m^2/s^3).
$\Delta\varphi$	Angular deviation (degree).
Ω	Angular velocity (rad/s).
ψ	Main-to-auxiliary rotors rotational speed ratio Ω_2/Ω_1.
ω	Specific turbulent dissipation rate ($1/s$).
Subscripts:	
f	Front.
max	Maximum.
r	Rear.
th	Theoretical.
Abbreviations:	
BEMT	Blade Element Momentum Theory.
DRWT	Double Rotor Wind Turbine.
MRF	Moving Reference Frame.
RANS	Reynolds-Averaged Navier-Stokes.
SRWT	Single-Rotor Wind Turbine.
SST	Shear Stress Transport.
TSR	Tip Speed Ratio.

1. Introduction

The dependence on wind turbines to meet diverse electricity demands prompts rapid development in wind turbine technologies. Notably, the Double Rotor Wind Turbine

(DRWT) setup, featuring an auxiliary rotor co-axially installed in front of the main rotor, is a promising technique to increase wind turbine power extraction. The Betz limit is the theoretical maximum efficiency for a wind turbine, conjectured by German physicist Albert Betz in 1919. According to Betz's limit, no windmill of any mechanism can capture more than 16/27 (59.3%) for the horizontal-axis wind turbines from the kinetic energy in the wind; thus, the factor 16/27 (59.3%) is known as Betz's limit coefficient. However, in practical terms, utility-scale wind turbines achieve a peak of 75–80% of the Betz limit. Newmann [1] determined the maximum theoretical power coefficient that can be attained from a DRWT as $C_{Pth-max} = 16/25 = 64\%$. In which this value is 4.74% higher than the maximum theoretical power coefficient of the single-rotor wind turbine (SRWT). Subsequently, several research papers focused on analysing the critical design parameters as: the diameter ratio $DR = D_f/D_r$ (the ratio between the front and the rear rotors' diameters), the spacing ratio $SR = X/D_f$ (the ratio between the distance between the two rotors and the front rotor diameter) the rotor's pitch angle θ (the angle between the blade tip chord line and the plane of rotation) and the rotors' relative rotational speed $\psi = \Omega_r/\Omega_f$ (the ratio between the rear and the front rotors' rotational speeds). The direction of rotation was also considered, as the front-rotor can rotate in the same direction as the rear-rotor (co-rotating) or in the opposite direction (counter-rotating). A further illustration of the mentioned parameters is shown in Figs. 1 and 2.

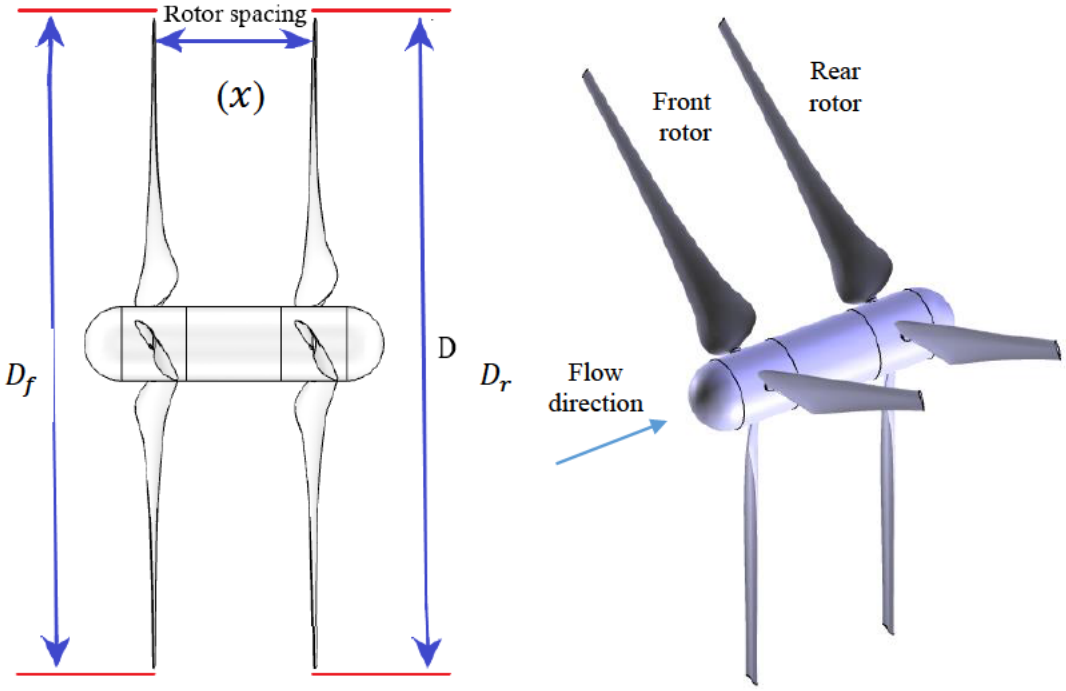

Fig. 1. Illustration of the double rotor wind turbine setup.

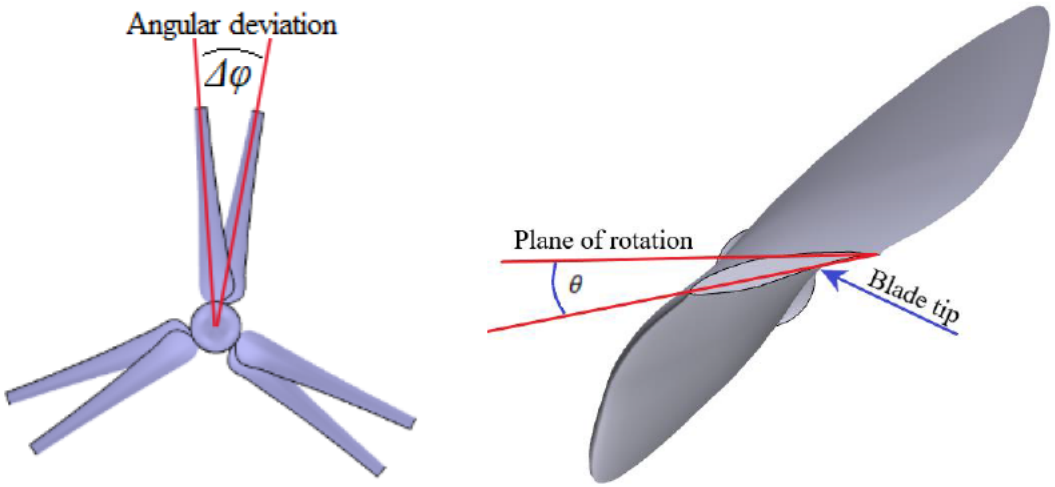

a) Angular deviation ($\Delta\varphi$). b) Blade pitch angle (θ).

Fig. 2. Illustration of the a) Azimuthal deviation. and b) Blade pitch angle.

The diameter ratio was identified as a significant parameter influencing turbine performance. Several studies stated the optimal value of the diameter ratio, suggesting either a $DR_{opt} = 0.5$ as in [2] or $DR_{opt} = 0.4$ as in [3] to achieve a higher average power coefficient. In contrast, the maximum power coefficient was proven to be attained at $DR = 1$ [4]. Furthermore, The variation in the power coefficient with the change in diameter ratio was explained in some studies [2], [3]. The diameter ratio was found to impact the power extraction of both rotors in distinct ways. Specifically, the decrease in the diameter ratio leads to a reduction in the power extraction of the front rotor, attributable to the reduction in the rotor area.

Conversely, the reduction in the diameter ratio facilitates an undisturbed influx of high-velocity air to reach the tip region of the rear rotor, increasing the power extraction of the rear rotor, effectively recapturing more power than that was lost by the front rotor area reduction, which enhances the overall turbine power extraction. However, the altered air flow pattern resulting from the effect of the stream tube divergence on the air leaving the front rotor impedes the undisturbed flux from approaching the rear rotor area in cases where the diameter ratio is near $DR = 1$. The mechanism that enhances the rear rotor power extraction does not present a fair compensation for the power lost by the front rotor area reduction at low diameter ratios.

The rotor spacing was demonstrated to slightly influence the turbine power coefficient, as highlighted in several studies [5] and [6], depending on the degree of rotor interaction. However, increasing the distance between rotors positively influenced the front rotor power extraction, primarily due to the reduced wake pressure reduction and the decreased rear rotor blockage. Conversely, this increase in the front rotor power extraction negatively impacts the rear rotor power extraction. This is attributed to the lower velocity air approaching the rear rotor. Eventually, the two effects were demonstrated to decline each other, and the total turbine power extraction slightly changed [6]. Additionally, some studies suggested a substantial increase in the turbine maximum power coefficient at $SR = 0.5$ [2] and [4].

One more parameter, the rear rotor blade pitch angle, was found to impact the turbine performance in several studies. For instance, Lee et al. [3] theoretically observed that the maximum turbine power extraction occurred when the front blade pitch angle was 6^o and the

rear rotor blade pitch angle was 0^o or 1^o. Also, Lee et al. [6] monitored the highest turbine power coefficient when both rotors' blade pitch angles were set to 0^o. Whereas Abdel Karim et al. [5] concluded that the rear rotor pitch angle has insignificant impact on the turbine performance within the range between 0^o and 2^o, assuming the front rotor blade pitch angle remained at 0^o. Moreover, maintaining the rear rotor pitch angle out of this range was found to negatively influence the turbine power coefficient. Regarding the rotors relative rotational speed, it was demonstrated that maintaining a lower rotational speed for the rear rotor improves the turbine power coefficient [3], [5] and [7]. This was attributed to the disturbed influx of low-velocity air reaching the rear rotor, reducing the angle of attack. Therefore, reducing the pitch angle was used to alleviate the reduction in the angle of attack.

The impact of the direction of rotation of the front rotor on the turbine performance was analysed in several studies. The turbine performance was enhanced with the counter-rotating configuration compared with the co-rotating configuration in terms of higher power coefficient and lower thrust coefficient [3], [4],[5], and [8]. This can be attributed to the larger angle of attack accompanied by the counter-rotating configuration. Consequently, the lift force direction is changed to have a large tangential component, generating more torque and increasing the turbine power extraction [9]. Hwang et al. [7] modified the rotors' diameters, the blades' twist, the chord distributions, and the rotational speeds of the rotors to enhance power performance. The modifications were conducted based on an optimization study that utilized the Multi-Island Genetic Algorithm, resulting in the achievement of a maximum power coefficient of $C_{Pmax} = 0.47$. Furthermore, the turbine power efficiency was improved by 90% by using a diameter ratio of $DR = 0.9$ and a rotational speed ratio of $\psi < 1$ at a wind velocity of 8 m/s. A summary of the standard research methodologies, the main considered parameters, and the main outputs of the mentioned studies is in Table. 1.

Table 1. Description of the main characteristics, methodologies, and output of a few DRWT studies.

Reference	Numerical method	Experimental method	Front diameter	Rear diameter	Wind velocity	Rotation direction	Concerned parameters	ΔC_P%
[2]	Quasi steady strip	Open field	5.5 m	11 m	variable	counter	$DR = 0.5$ $SR = 0.4$	21%
[3]	BEMT	-	variable	variable	-	counter	$DR = 0.5$ $\psi < 1$ $\theta_f = 6,$ $\theta_r = 1{,}0$	8.9%
[4]	RANS-$k-\varepsilon$	-	variable	0.944 m	-	counter	$DR = 1$ $SR = 0.5$	19.37%
[5]	RANS-$k-\omega$	-	0.9 m	0.9 m	10 m/s	Co-counter	SR $\theta_r = 0 - 2$ $\psi = 0.8$	20.27%
[6]	Free wake vortex lattice	-	4.5 m	4.5 m	-	counter	SR $\theta_f = 0$ $\theta_r = 0$	12%
[8]	-	2.4 m x 2.3 m wind tunnel	0.15 m	0.28 m	6.5 m/s	Co-counter	Direction of rotation (counter)	7.2%
[10]	BEMT	-	7.16 m	7.16 m	10 m/s	counter	-	$2-8$%

Several simplifications can be implemented for practical DRWT applications, such as utilizing co-rotating rotors with equal rotation speeds to facilitate construction. While extensive research has focused on the impact of various geometrical parameters on DRWT performance, little attention has been given to studying the effect of the azimuthal deviation $\Delta\varphi$ between the rotors in the co-rotating equal-speed DRWT configuration. The azimuthal deviation describes the angle between the azimuthal positions of the front and rear rotors, as shown in Fig. 1. In this paper, a co-rotating DRWT utilizing two identical rotors rotating at the same speed is numerically modelled and studied concerning the Azimuthal deviation $\Delta\varphi$ between rotors in the range from $\Delta\varphi = -15$ to $\Delta\varphi = +15$. The adopted small-scale turbine has a diameter of 0.9 m with two spacing ratios of $SR = 0.14$ and $SR = 0.25$. The study aims to elucidate the power coefficient performance under various configurations of azimuthal deviation and spacing ratios.

2. Methods and Tools

2.1 Model Geometry

The base case DRWT model was built using two identical rotors of the 0.9 m diameter, as it was designed by Krogstad and Lund [11] for a SRWT. The 3-bladed rotor, with blade chord and twist angle distributions depicted in Fig. 3 and Fig. 4, was designed for a SRWT operating in a rated wind velocity of 10 m/s and a $TSR = 6$. For the DRWT study, the rotor was replicated for $DR = 1$ with two spacing ratios of $SR = 0.14$ and $SR = 0.25$. The study adopted a blade pitch angle of $\theta = 0^o$, and equal rotating speed ($\psi = 1$) for both rotors. The rotors were installed with various deviation angles ranging between $\Delta\varphi = -15$ and $\Delta\varphi = +15$ during the study and with $\Delta\varphi = 0$ during validation.

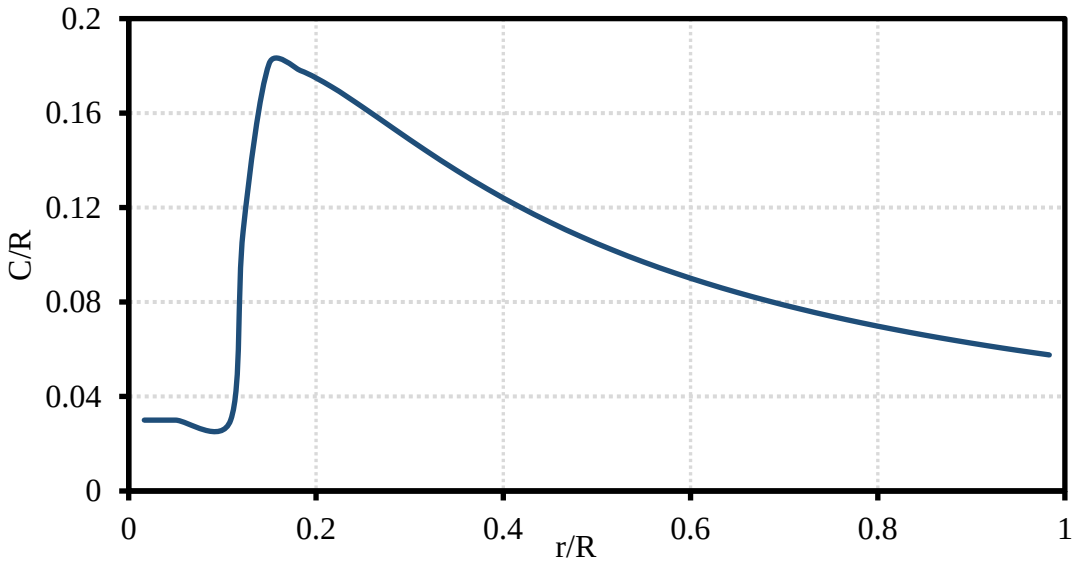

Fig. 3. Blade chord distribution [11].

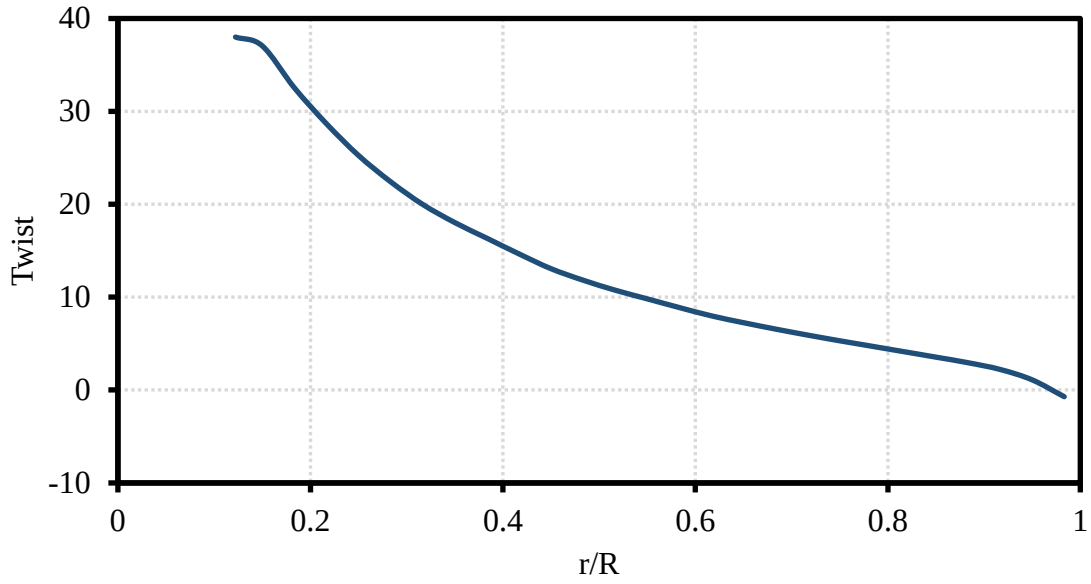

Fig. 4. Blade twist distribution [11].

2.2 Numerical method

The Multiple Reference Frame (MRF) method was adopted to simulate Rotors' rotation. Two side-by-side rotating inner domains around the two rotors were used in the DRWT cases, while a single inner domain was used in the SRWT case. The interaction between the two rotors' flow fields was simulated by assigning an interface boundary condition at the separating surfaces. A stationary outer domain wrapping the two inner rotating domains was built with no-slip boundary conditions assigned for its cylindrical outer face. An inlet velocity of 10 m/s was imposed at the domain inlet boundary condition, while atmospheric pressure was assumed at the domain outlet. The axial and radial dimensions of the cylindrical global domain were chosen as $12R$ and $5R$, respectively. The selection of radius $5R$ was based on a domain-independence test conducted by Abdel Karim et al. [5], representing a larger flow area than the area of the wind tunnel where the reference turbine was tested [11]. The inlet and outlet planes are located at distances of $2R$ and $10R$ before and after the front rotor location, respectively. The inner rotating domain radius and thickness was assumed to be $1.333R$ and $0.45R$ based on [5]. Domains dimensions are depicted in Fig. 5.

For a reduced calculation cost and time, only one-third of the physical domain was modelled using periodic planes. The proposed domains and their boundary surfaces are shown in Fig. 5. The second-order upwind scheme was used to descritatztion the convective terms in the solved equations using the ANSYS FLUENT pressure-based algorithm. The RANS model was employed to simulate the flow field around the turbine. Whereas $k-\omega$ Shear Stress Transport (SST) was used to model turbulence stresses. The combination was proved to have good accuracy in capturing and quantifying the mean flow characteristics such as the turbine power and thrust [5], [11]–[13].

2.3. Grid Meshing

A hexahedral structured Grid was utilized throughout the global domain for higher accuracy and lower calculation time and cost. The distribution of the grid along the domain's boundaries and the blade surface can be observed in Figs. 6 and 7, respectively. The total

number of grids was determined using a grid-independence test applied to the SRWT case, ensuring the stability of the calculation results without significant variations as the number of cells increased. The power and thrust coefficients remained relatively stable beyond 4.5 million cells, exhibiting marginal changes of 0.003% and 0.1%, respectively, as shown in Fig. 8.

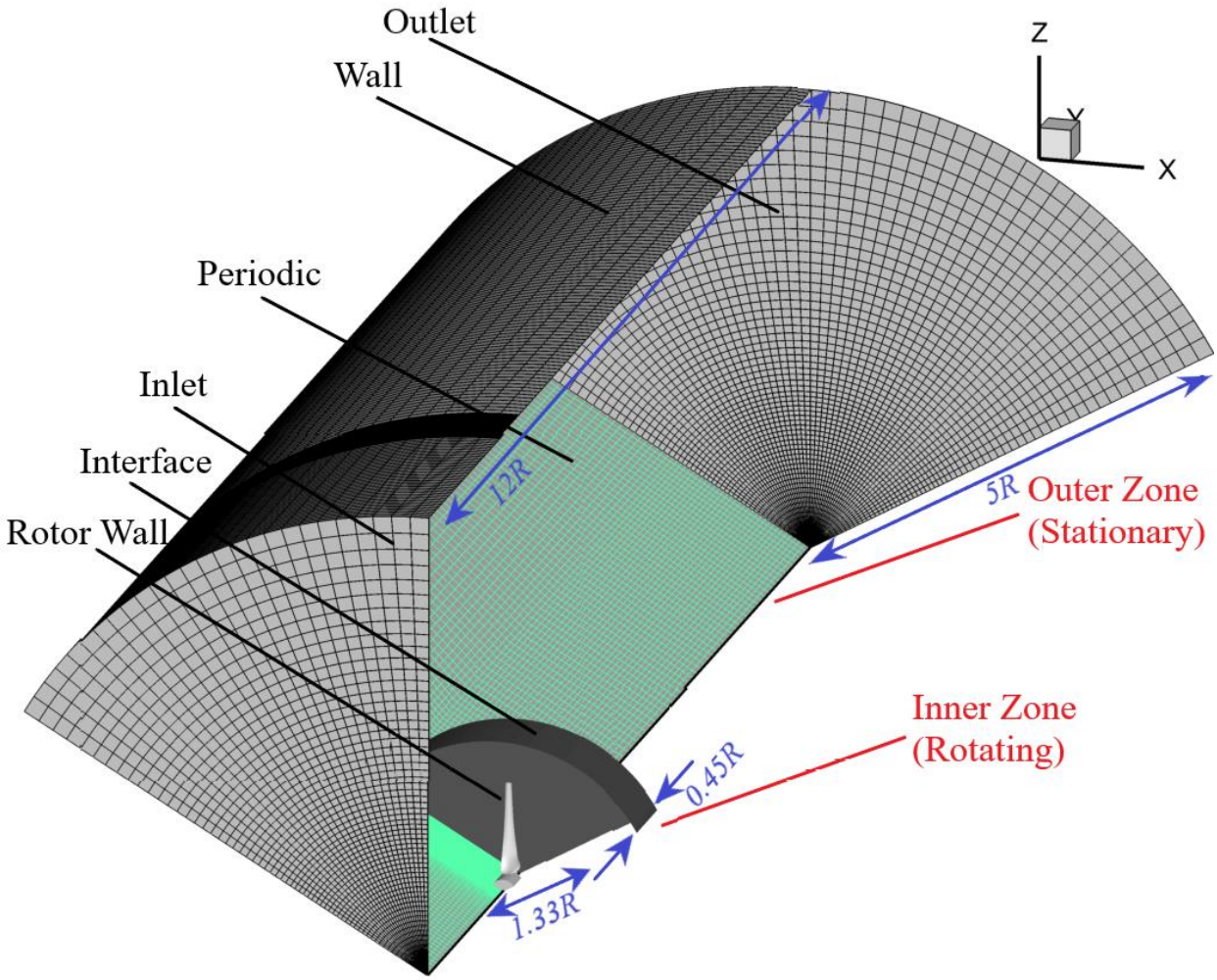

Fig. 5. Illustration of the domains and boundary zones.

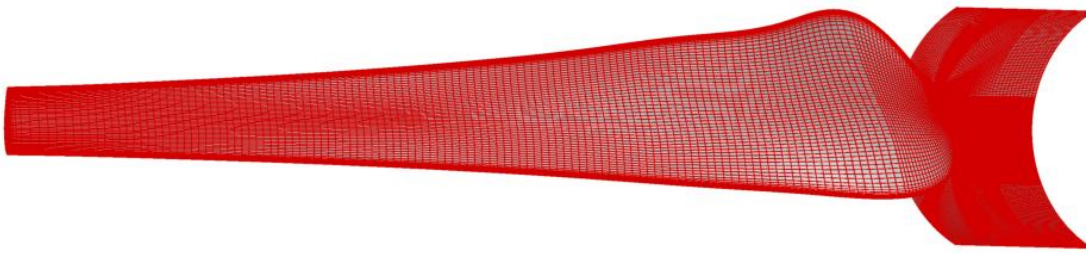

Fig. 6. Grid shape on the blade surface.

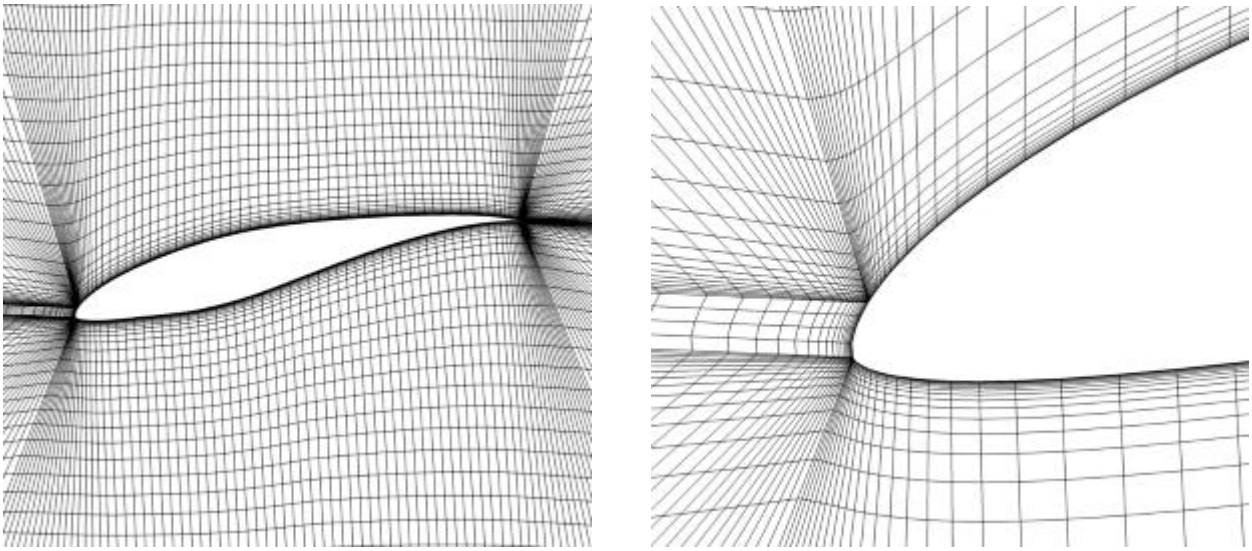

a) Airfoil. b) Airfoil leading edge

Fig. 7. Grid shape at blade mid-span airfoil and its leading edge.

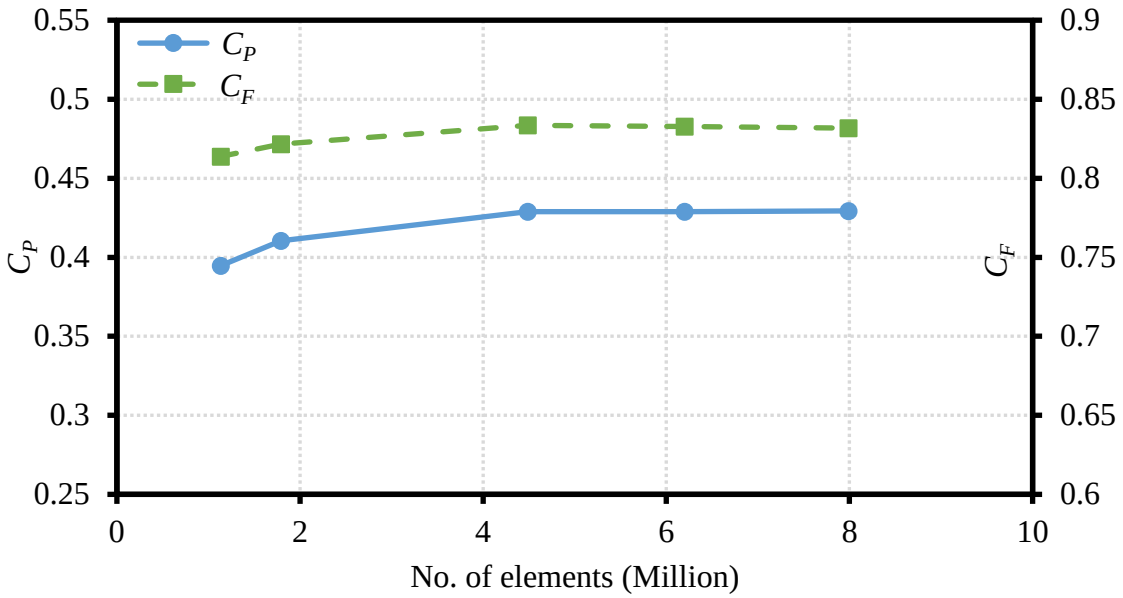

Fig. 8. SRWT Power and thrust coefficients variation with the number of cells at $TSR = 6$.

3. Model validation

The model validation process was performed in two stages; the first one was to validate SRWT results against the experimental and numerical data obtained by Krogstad and Lund [11], while the second was to validate the proposed DRWT model against the data obtained by Abdel Karim et al. [5]. Fig. 9 shows the validation of SRWT results regarding the power and thrust coefficient variation with the TSR. The power and thrust coefficients from the present study are observed to agree with the benchmark data. The most significant discrepancy is found at $TSR = 4$ with 4.4% and 5.1% deviation for the power and thrust coefficients, respectively. The DRWT validation data is shown in Fig. 10. The two curves of power coefficient variation against TSR from present study and Abdel Karim et al. [5] are

observed to be in a good matching with a most significant deviation percentage of 5% at $TSR = 4$.

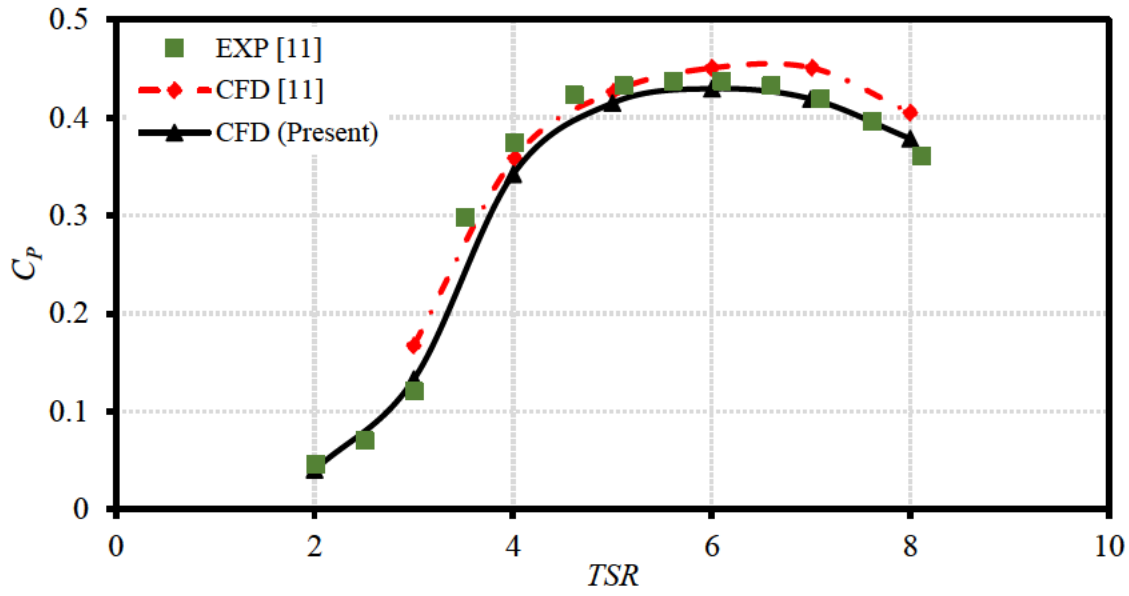

a) Power coefficient

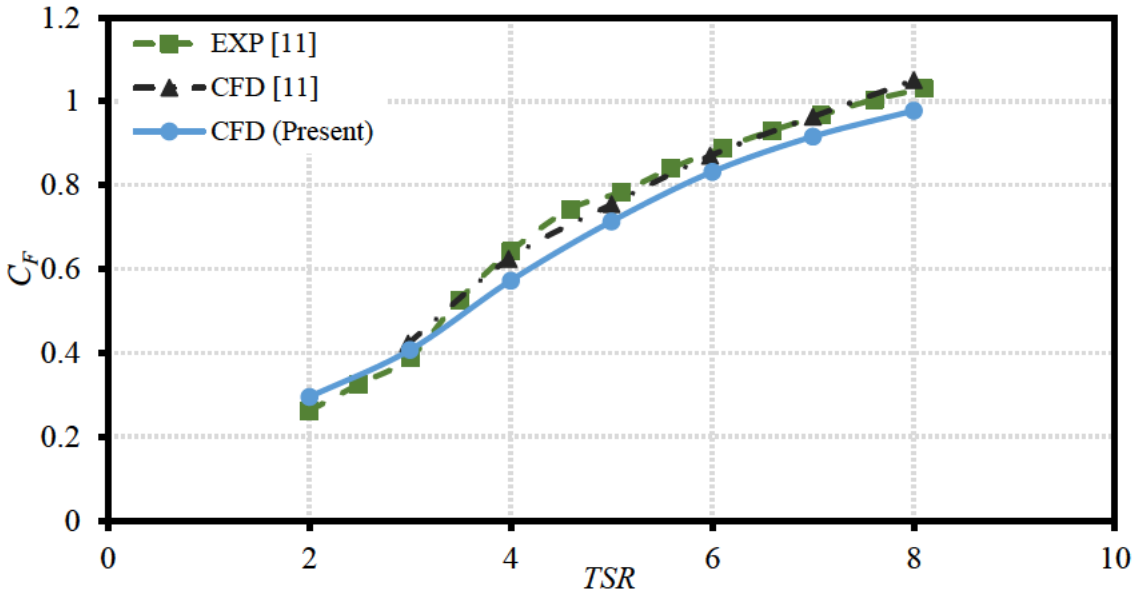

b) Thrust coefficient

Fig. 9. Comparison between the power and thrust coefficients variation with TSR obtained from the present study SRWT and the benchmark data of [11].

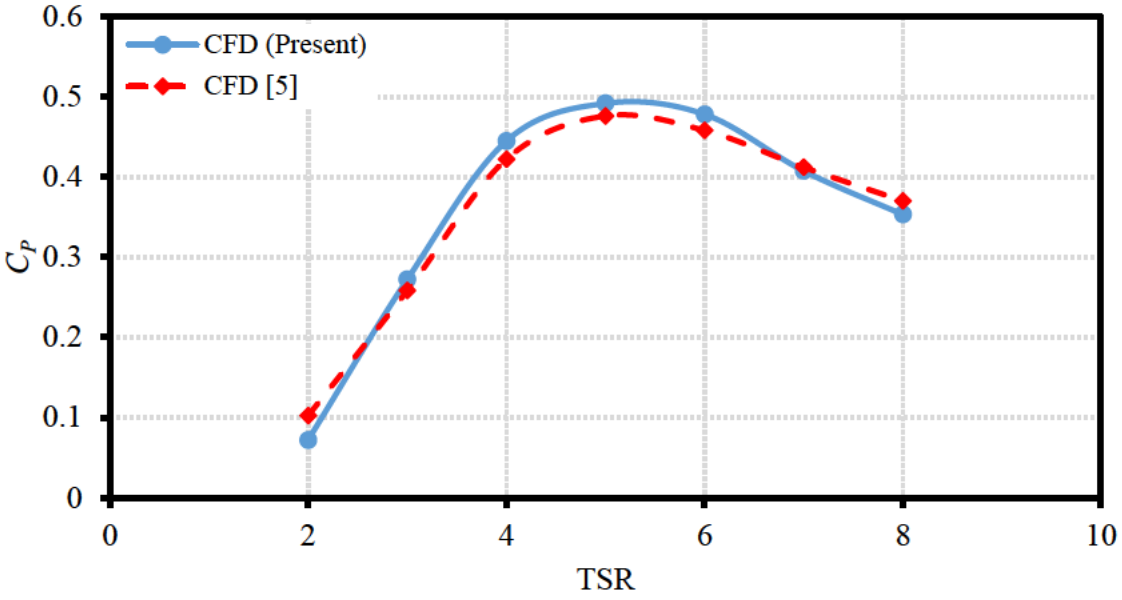

Fig. 10. Comparison between the DRWT power coefficient variation with the TSR obtained from the present study and the benchmark data of [5].

4. Results and discussion

This section presents the investigation of the effect of the azimuthal deviation $\Delta\varphi$ on the power coefficient of the DRWT. Two rotor spacings SR were considered: 0.14 and 0.25. The consideration of the two spacings aims to determine the effect of varying distances between rotors and different azimuthal deviation configurations. The range of the Azimuthal deviation considered was from -15^o to $+15^o$, where the positive sign signifies the angular lead of the front rotor over the rear rotor in the direction of rotation, and the negative sign indicates the angular lead of the rear rotor over the front rotor in the direction of rotation. Comparison between the seven azimuthal deviations in terms of the power and thrust coefficients variation with TSR in the two rotor spacing cases are shown in Fig. 11 and Fig. 12, respectively, compared to SRWT curves. Figures reveal no significant differences in the power coefficient across the seven azimuthal deviations throughout the entire range of TSR in both cases. In contrast, the maximum increase in the power coefficient over the SRWT was observed to be 15% at $SR = 0.14$ and $TSR = 5$. The turbine's overall power coefficient was not affected by the variation of the azimuthal deviations; therefore, the performance of the power coefficient of each rotor is discussed in detail for the two rotor spacing cases, giving special attention to the tip speed ratios of $TSR = 4$, $TSR = 5$, and $TSR = 6$.

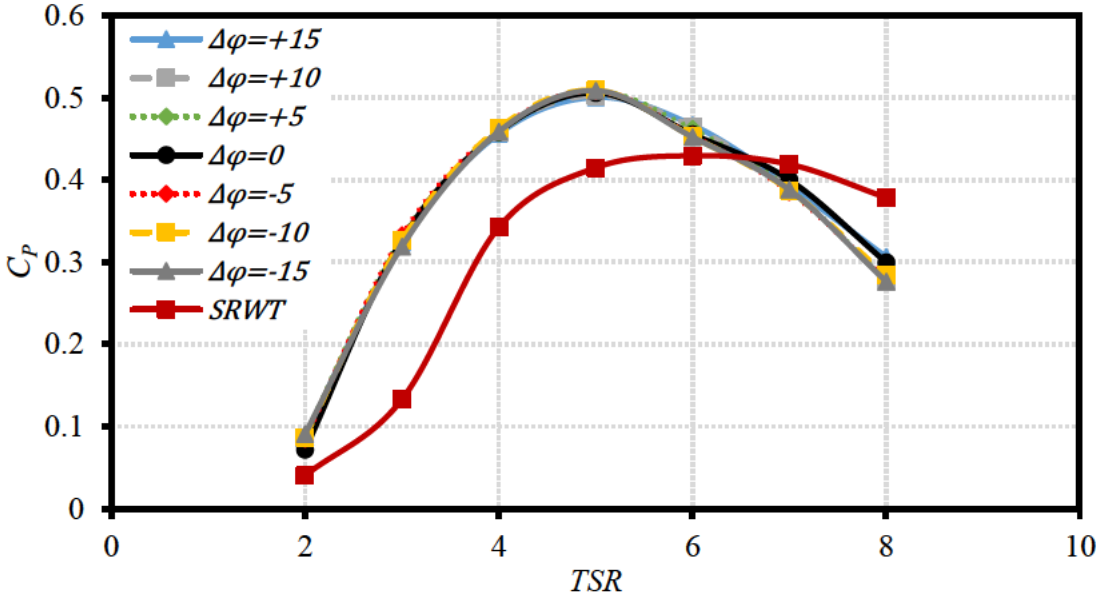

Fig. 11. Comparison between the power coefficient of the seven azimuthal deviations and the SRWT against TSR in the case of $SR = 0.14$.

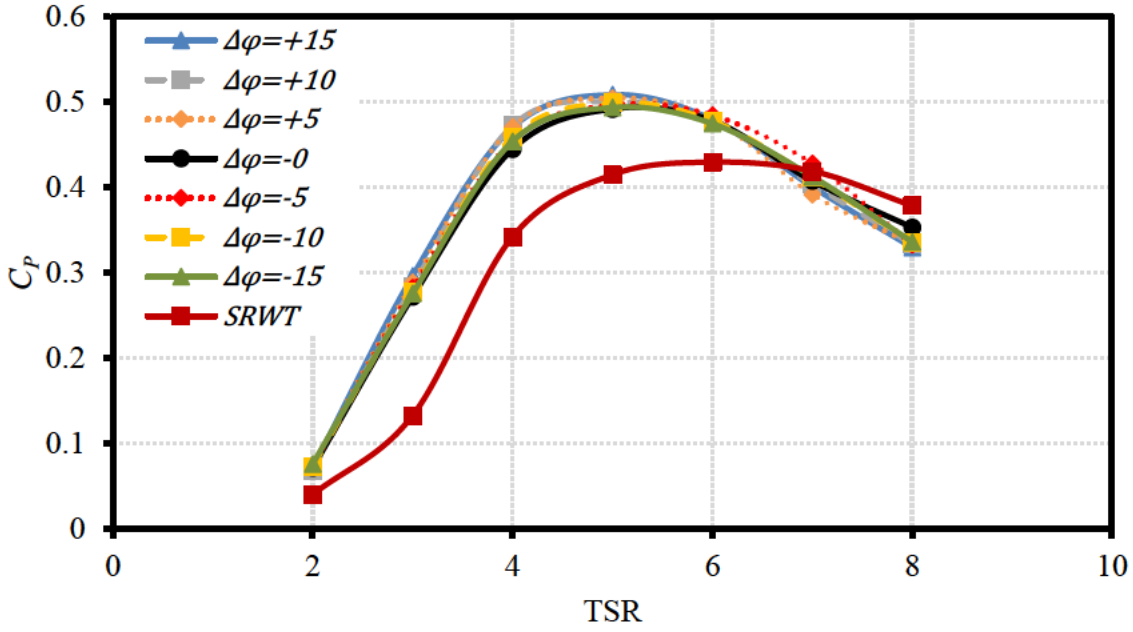

Fig. 12. Comparison between the power coefficient of the seven azimuthal deviations and the SRWT against TSR in the case of $SR = 0.25$.

4.1. Case I: SR=0.14

The front rotor, the rear rotor, and the total turbine power coefficients are plotted against the angular deviation at $TSR = 4$, $TSR = 5$, and $TSR = 6$ in Figs 13, 14, and 15, respectively. For the three TSRs, the power coefficient of the front rotor increases with the increase of angular deviation in the positive direction, while the rear rotor power coefficient increases with the increase of the angular deviation in the negative direction. The maximum changes in the power coefficient of the front rotor at the three TSRs are $\Delta C_{P4} = 0.035$, $\Delta C_{P5} = 0.058$, and $\Delta C_{P6} = 0.058$, while the maximum changes in the power coefficient of the rear rotor are $\Delta C_{P4} = -0.036$, $\Delta C_{P5} = -0.066$, and $\Delta C_{P6} = -0.043$. The counteractive effects offset each

other, minimally impacting the overall turbine power coefficient. The main role of this behavior may be related to the rear rotor. As shown in Fig. 16a, positioning the rear rotor ahead of the front rotor (with respect to azimuth angle) in the direction of rotation minimizes direct disturbance of the approaching air by the front rotor. Thus, the air flows smoother with a slight reduction in the angle of attack compared to the case of $\Delta\varphi = 0$ where the rear rotor blade is aligned behind the front one, which increases the rear rotor power extraction. The increase in the power extraction of the rear rotor enhances flow blockage and subsequently increases the pressure in the central region between the two rotors, as illustrated in Fig. 17a. This increase in pressure reduces the power extraction by the front rotor.

Conversely, positioning the rear rotor behind the front rotor (with respect to azimuth angle) in the direction of rotation intensifies the direct disturbance of the approaching air by the front rotor, as depicted in Fig. 16b. Consequently, this configuration leads to a reduction in the angle of attack of the airflow compared to the $\Delta\varphi = 0$ case, resulting in a reduction in the power extraction of the rear rotor. The rear rotor power reduction subsequently reduces the pressure in the central region between the rotors, as illustrated in Fig. 17b, leading to increased power extraction by the front rotor. For a better understanding of the effect of the azimuthal deviation on the flow field approaching the rear rotor, the velocity triangles of the flow approaching the rear rotor blade mid-span are compared for the cases of $\Delta\varphi = -15$ and $\Delta\varphi = +15$ in Fig. 18. The comparison reveals a higher relative flow angle for the case of $\Delta\varphi = -15$, resulting in a corresponding higher angle of attack. Furthermore, as depicted in Fig. 19, the air flows smoothly around the blade in both cases. This smoothness indicates that the angle of attack is within a proper range, minimizing the risk of separation occurrence.

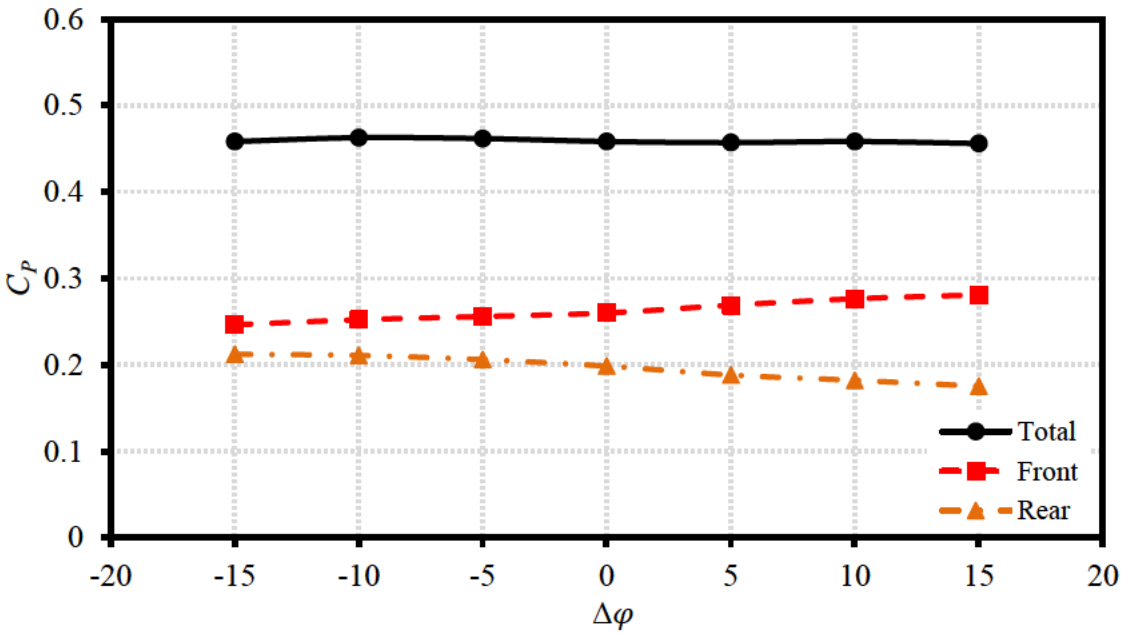

Fig. 13. Power coefficient variation of the front rotor, the rear rotor, and the total turbine with the azimuthal deviation at $TSR = 4$ and $SR = 0.14$.

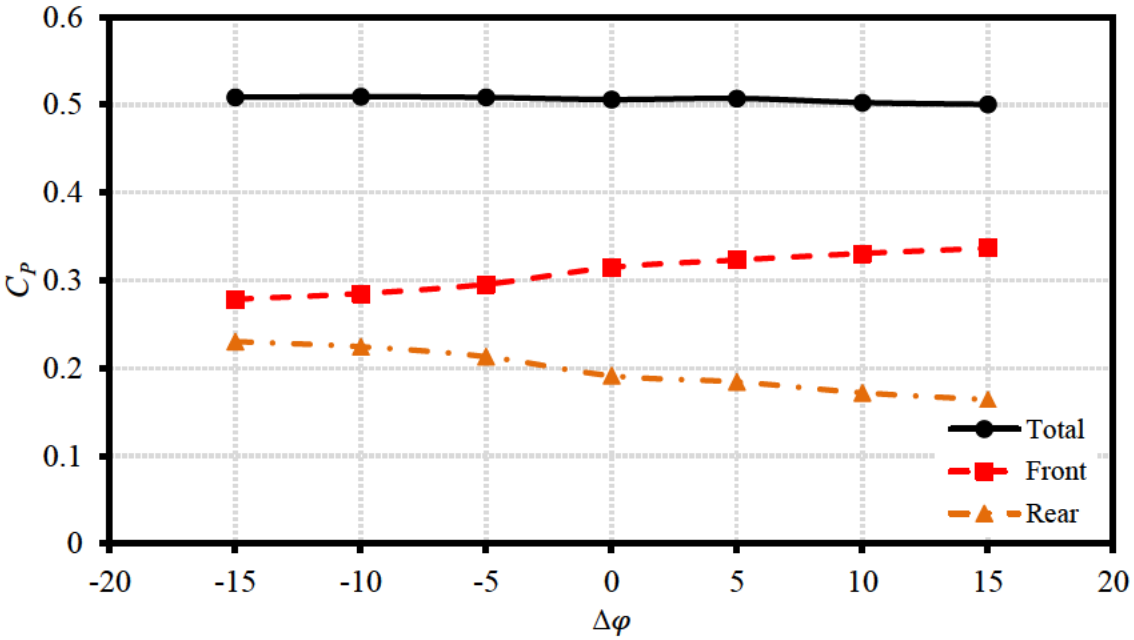

Fig. 14. Power coefficient variation of the front rotor, the rear rotor, and the total turbine with the azimuthal deviation at $TSR = 5$ and $SR = 0.14$.

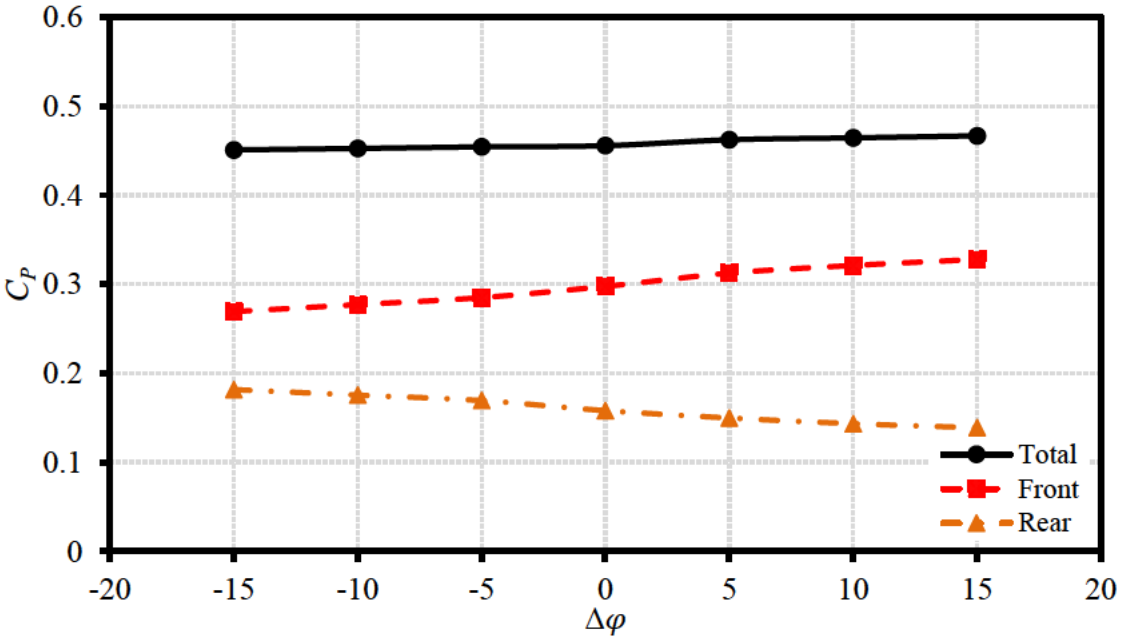

Fig. 15. Power coefficient variation of the front rotor, the rear rotor, and the total turbine with the azimuthal deviation at $TSR = 6$ and $SR = 0.14$.

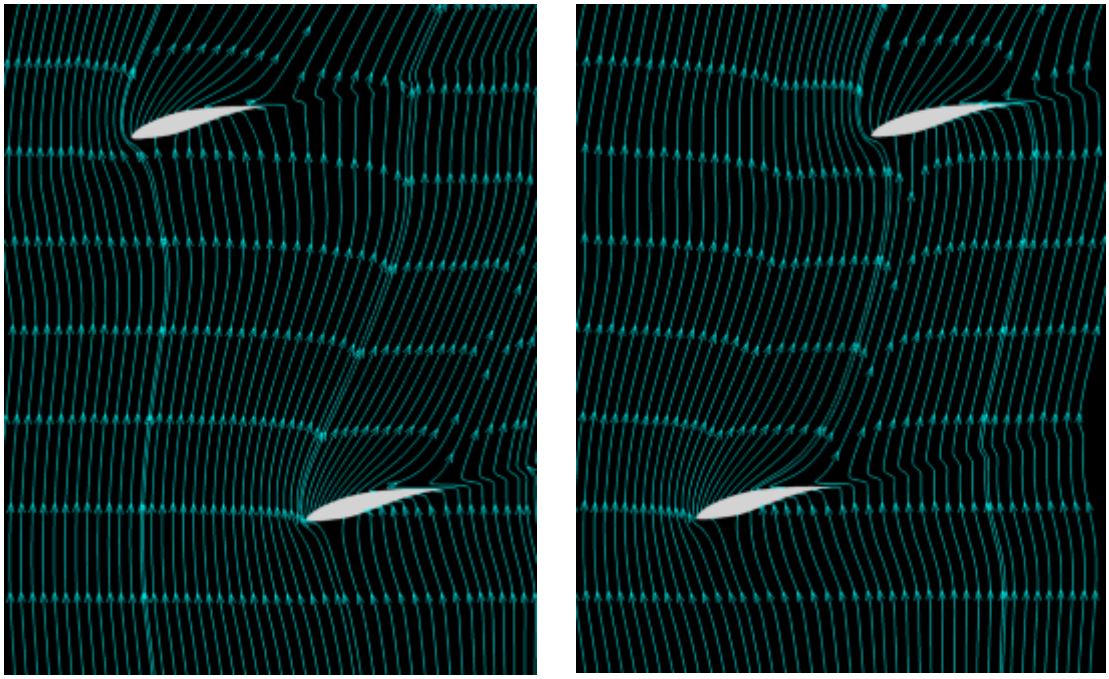

a) $\Delta\varphi = -15$ b) $\Delta\varphi = +15$

Fig. 16. Absolute flow passage from the front rotor to the rear rotor blades at a) $\Delta\varphi = -15$ and b) $\Delta\varphi = +15$ at $TSR = 5$.

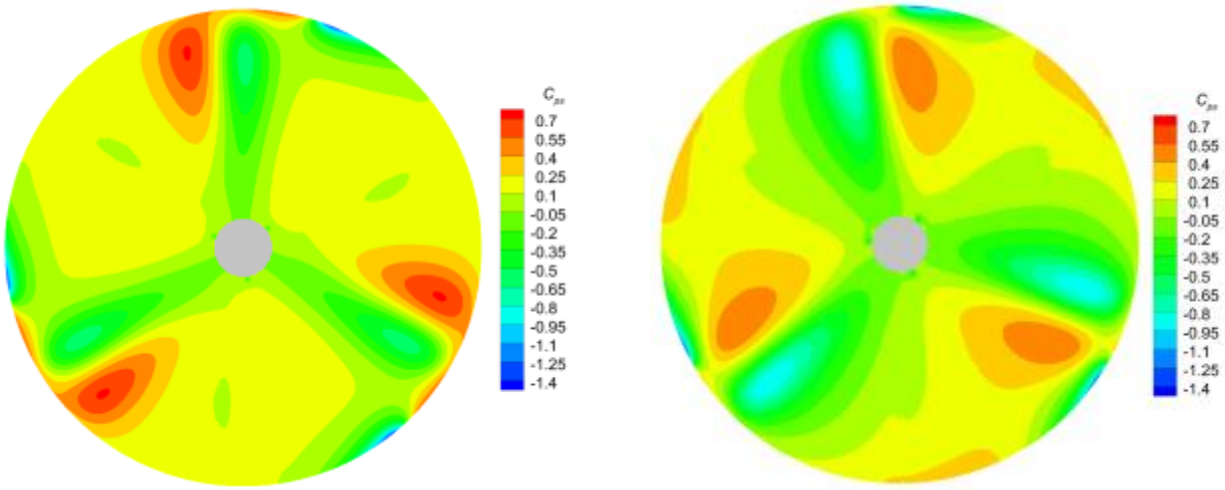

a) $\Delta\varphi = -15$ b) $\Delta\varphi = +15$

Fig. 17. Pressure coefficient in the mid-distance between the front and rear rotors for the angular deviations of a) $\Delta\varphi = -15$ and b) $\Delta\varphi = +15$ at $TSR = 5$.

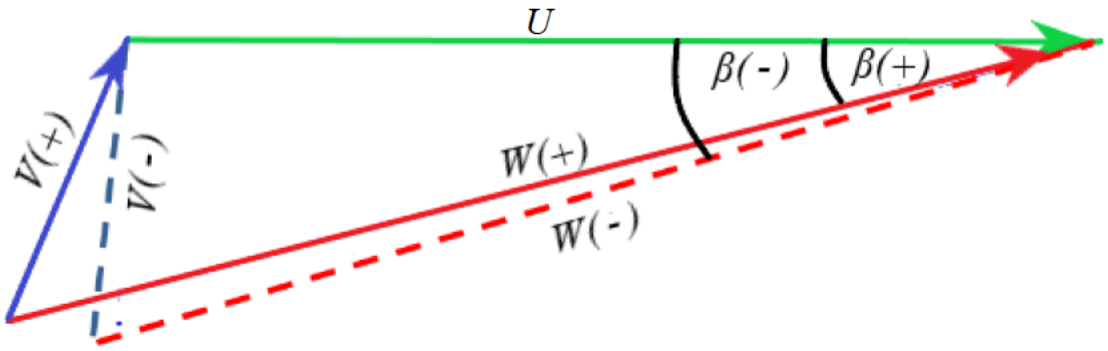

Fig. 18. Comparison between the velocity triangles of the air approaching the mid-span of the rear rotor blade at $\Delta\varphi = -15$ referred by $(-)$ and $\Delta\varphi = +15$ referred by $(+)$ at $SR = 0.14$ and $TSR = 5$.

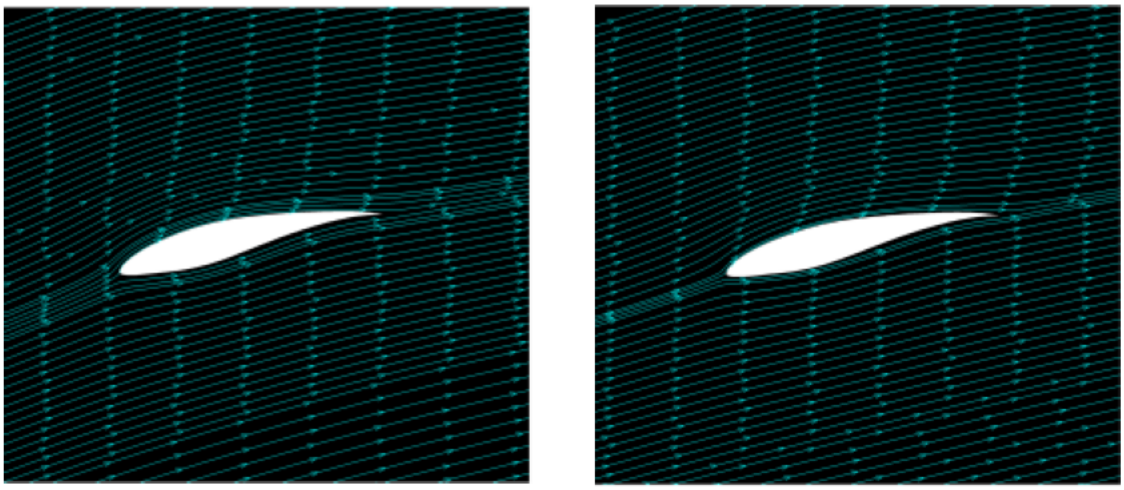

a) $\Delta\varphi = -15$ b) $\Delta\varphi = +15$

Fig. 19. Streamlines around the mid-span of the rear rotor blade for a) $\Delta\varphi = -15$ and b) $\Delta\varphi = +15$ at $SR = 0.14$ and $TSR = 5$, with arrow referring to the direction of the relative velocity.

4.2. Case II: SR=0.25

The front rotor, the rear rotor, and the total turbine power coefficients are plotted against the azimuthal deviation at $TSR = 4$, $TSR = 5$, and $TSR = 6$ in Figs 2٠, 2١ and 2٢, respectively. The Figures indicate a minimal influence of the azimuthal deviation on the power coefficient of the front rotor, the rear rotor, and the total turbine at the three TSRs. The maximum changes in the power coefficient of the front rotor at the three TSRs are $\Delta C_{P4} = 0.007$, $\Delta C_{P5} = 0.005$, and $\Delta C_{P6} = 0.002$, while the maximum changes in the power coefficient of the rear rotor are $\Delta C_{P4} = 0.009$, $\Delta C_{P5} = 0.009$, and $\Delta C_{P6} = 0.005$. The insignificant impact of the azimuthal deviation on the power coefficient of both rotors can be attributable to the increased separating distance, which allows the flow to slightly redirect itself to attain proper angle of attack approaching the rear rotor (Fig. 23). Additionally, the increased separating distance facilitates the recovery of flow pressure, promoting uniformity and reduction in the pressure ahead of the rear rotor, as depicted in Fig. 24, which contributes to the reduction of the impact of the azimuthal deviation.

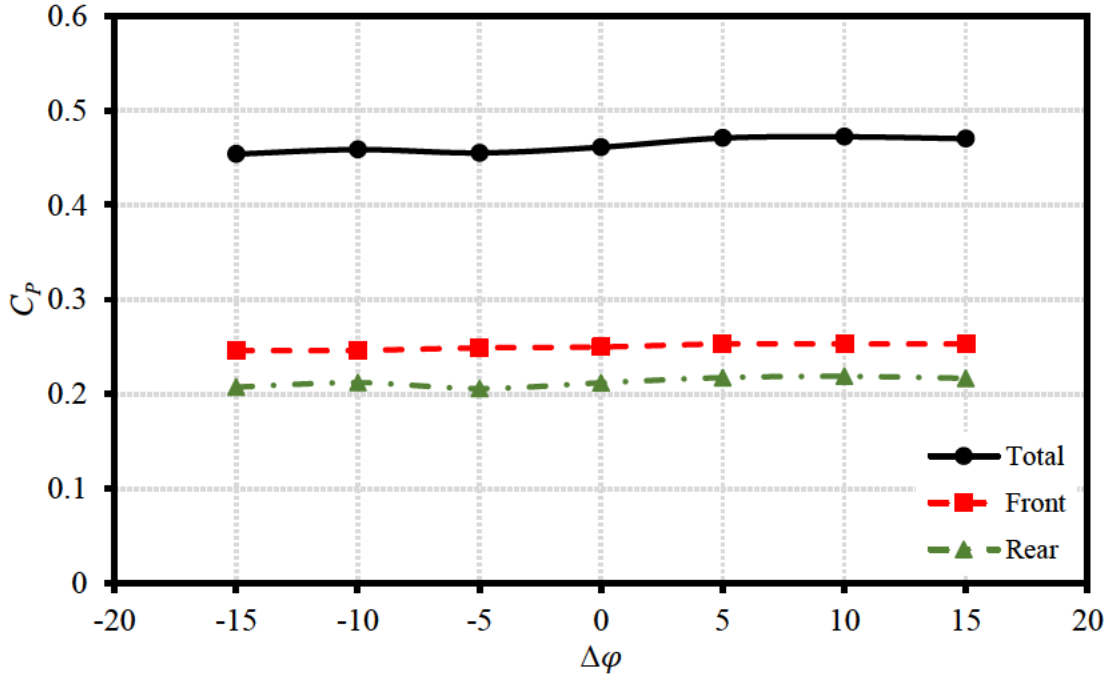

Fig. 20. Power coefficient variation of the front rotor, the rear rotor, and the total turbine with the azimuthal deviation at $TSR = 4$ and $SR = 0.25$.

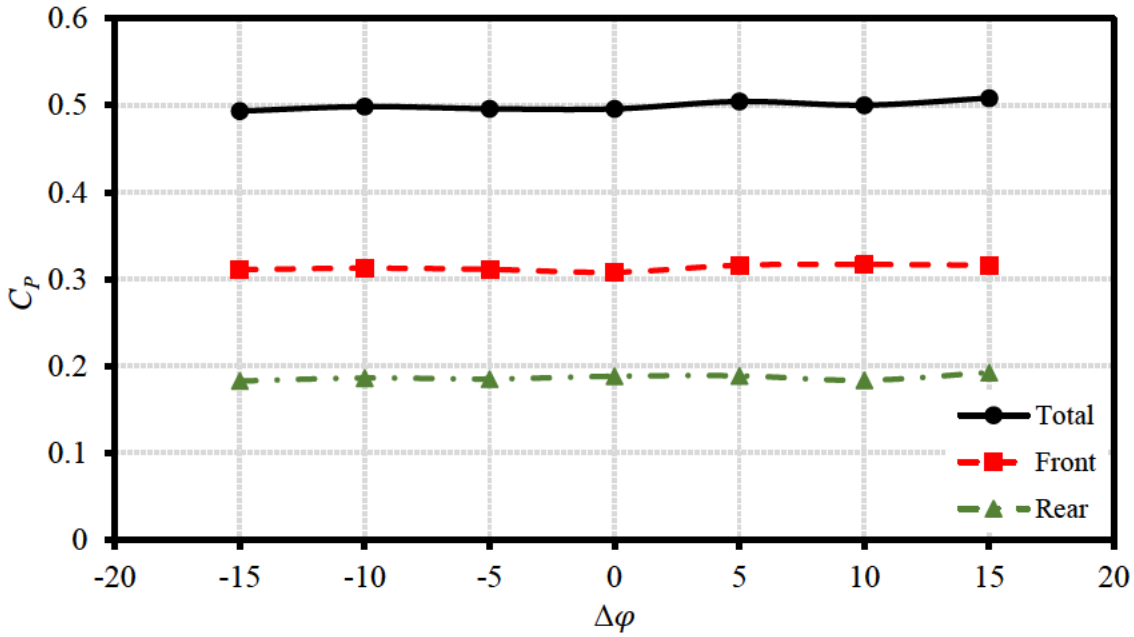

Fig. 21. Power coefficient variation of the front rotor, the rear rotor, and the total turbine with the azimuthal deviation at $TSR = 5$ and $SR = 0.25$.

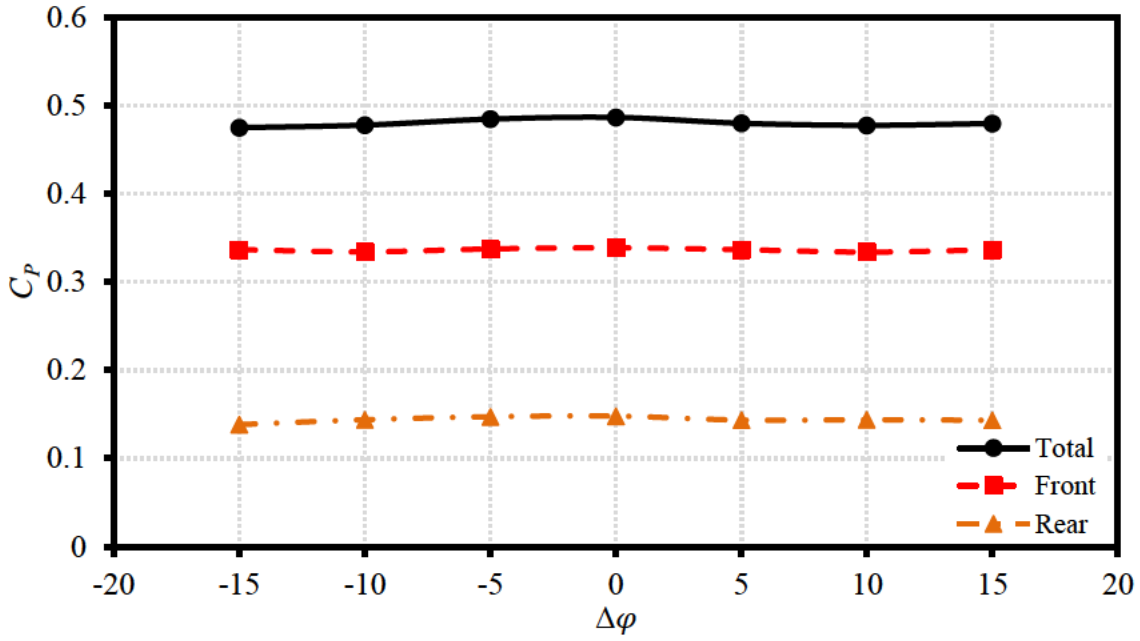

Fig. 22. Power coefficient variation of the front rotor, the rear rotor, and the total turbine with the angular deviation at $TSR = 6$ and $SR = 0.25$.

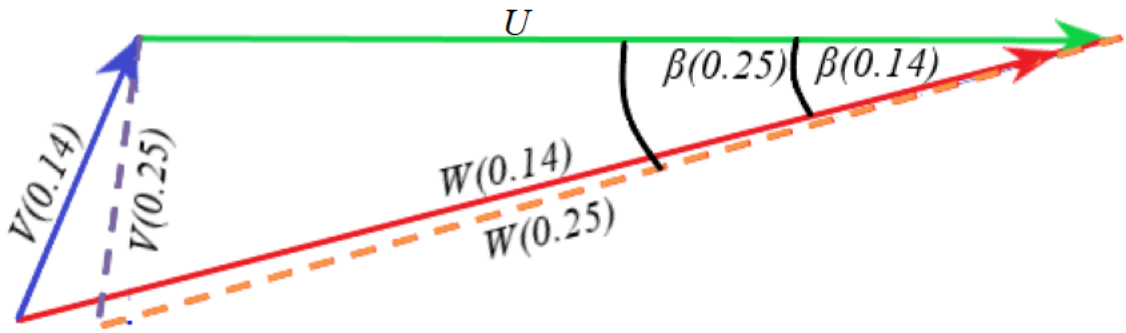

Fig. 23. Comparison between the velocity triangles of the air approaching the mid-span of the rear rotor blade at $SR = 0.14$ referred by (0.14) and $SR = 0.25$ referred by (0.25) at $\Delta\varphi = +15$ and $TSR = 5$.

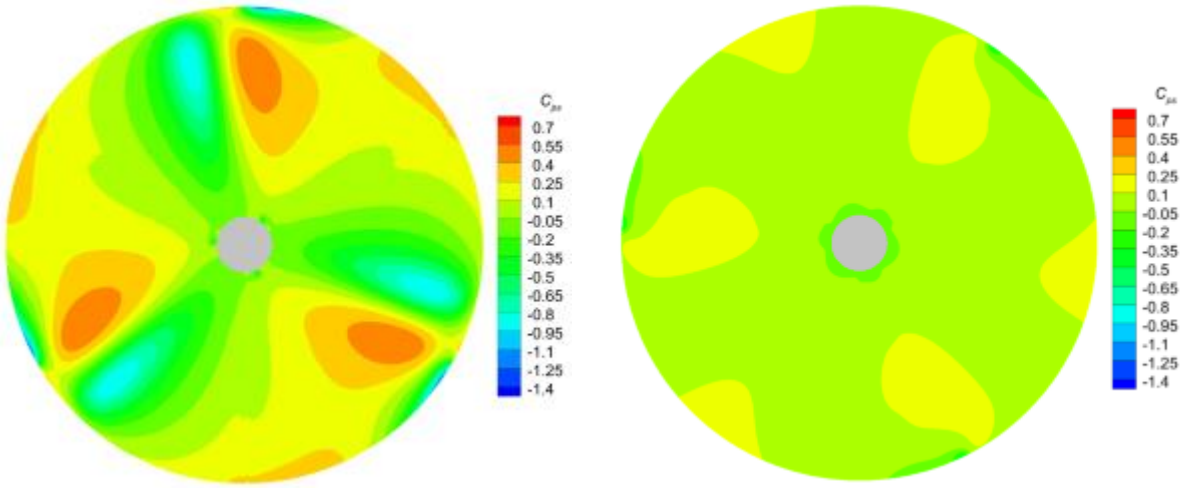

a) $SR = 0.14$ b) $SR = 0.25$

Fig. 24. Pressure coefficient distribution in the mid-distance between the front and rear rotors of $\Delta\varphi = +15$ with rotor spacing of a) $SR = 0.14$ and b) $SR = 0.25$ at $TSR = 5$.

5. Conclusions

The effect of azimuthal deviation on the performance of a DRWT was investigated in this study. The results suggested that the azimuthal deviation has no remarkable impact on the overall turbine power coefficient with a change in the maximum power coefficient by $\Delta C_P = 0.008$ at $SR = 0.14$ and $\Delta C_P = 0.014$ at $SR = 0.25$ at the optimal $TSR = 5$. This slight effect was attributed to distinct reasons in the two considered rotor spacing cases. At $SR = 0.14$, representing the small distance between rotors, the angular deviation was found to have a contrasting effect on the front and the rear rotors. The maximum change in the power coefficients of the front and rear rotors was $\Delta C_P = 0.058$ and $\Delta C_P = 0.066$. As azimuthal deviation increased from negative to positive value, the power extraction by the rear rotor increased because it was exposed to a less disturbed flow, which increased the angle of attack and power extraction. Also, a relatively high-pressure region is created in front of the rear rotor, which decreases the front rotor power extraction. The net extracted power from the front and rear remained almost consistent, as the positive and negative effects of the azimuthal deviation almost declined each other. At $SR = 0.25$, representing the significant distance, the increased distance between the two rotors facilitated flow recovery, resulting in almost the same power coefficients for both rotors at different azimuthal deviations and, consequently, the same total power extracted by the DRWT. Eventually, the highest increase in the maximum power coefficient over the SRWT was indicated to be 15% at $TSR = 5$.

References

[1] B. . Newman, “Multiple actuator-disc theory for wind turbines,” *J. Wind Eng. Ind. Aerodyn.*, vol. 24, no. 3, pp. 215–225, Oct. 1986, doi: 10.1016/0167-6105(86)90023-1.

[2] S. N. Jung, T. S. No, and K. W. Ryu, “Aerodynamic performance prediction of a 30 kW counter-rotating wind turbine system,” *Renew. Energy*, vol. 30, no. 5, pp. 631–644, 2005, doi: 10.1016/j.renene.2004.07.005.

[3] S. Lee, H. Kim, E. Son, and S. Lee, “Effects of design parameters on aerodynamic performance of a counter-rotating wind turbine,” *Renew. Energy*, vol. 42, pp. 140–144, 2012, doi:

10.1016/j.renene.2011.08.046.

[4] V. A. Koehuan, Sugiyono, and S. Kamal, "Investigation of counter-rotating wind turbine performance using computational fluid dynamics simulation," *IOP Conf. Ser. Mater. Sci. Eng.*, vol. 267, no. 1, pp. 0–9, 2017, doi: 10.1088/1757-899X/267/1/012034.

[5] H. A. Abdel Karim, A. R. El-Baz, N. A. Aziz Mahmoud, and A. M. Hamed, "Numerical analysis on the performance of Dual Rotor wind turbine," *Int. J. Sci. Res. Manag.*, vol. 8, no. 03, pp. 352–368, 2020, doi: 10.18535/ijsrm/v8i03.ec02.

[6] S. Lee, E. Son, and S. Lee, "Velocity interference in the rear rotor of a counter-rotating wind turbine," *Renew. Energy*, vol. 54, pp. 235–240, 2013, doi: 10.1016/j.renene.2012.08.003.

[7] B. Hwang, S. Lee, and S. Lee, "Optimization of a counter-rotating wind turbine using the blade element and momentum theory," *J. Renew. Sustain. Energy*, vol. 5, no. 5, 2013, doi: 10.1063/1.4826940.

[8] Z. Wang, A. Ozbay, W. Tian, and H. Hu, "An experimental study on the aerodynamic performances and wake characteristics of an innovative dual-rotor wind turbine," *Energy*, vol. 147, pp. 94–109, 2018, doi: 10.1016/j.energy.2018.01.020.

[9] W. Yuan, W. Tian, A. Ozbay, and H. Hu, "An experimental study on the effects of relative rotation direction on the wake interferences among tandem wind turbines," *Sci. China Physics, Mech. Astron.*, vol. 57, no. 5, pp. 935–949, 2014, doi: 10.1007/s11433-014-5429-x.

[10] A. D. Hoang and C.-J. Yang, "Design and Performance Evaluation of a 10kW Scale Counter-Rotating Wind Turbine Rotor," *J. Korean Soc. Mar. Environ. Saf.*, vol. 20, no. 1, pp. 104–112, 2014, doi: 10.7837/kosomes.2014.20.1.104.

[11] P.-Å. Krogstad and J. A. Lund, "An experimental and numerical study of the performance of a model turbine," *Wind Energy*, vol. 15, no. 3, pp. 443–457, Apr. 2012, doi: 10.1002/we.482.

[12] M. H. Lee, Y. C. Shiah, and C. J. Bai, "Experiments and numerical simulations of the rotor-blade performance for a small-scale horizontal axis wind turbine," *J. Wind Eng. Ind. Aerodyn.*, vol. 149, pp. 17–29, 2016, doi: 10.1016/j.jweia.2015.12.002.

[13] J. O. Mo and Y. H. Lee, "CFD Investigation on the aerodynamic characteristics of a small-sized wind turbine of NREL PHASE VI operating with a stall-regulated method," *J. Mech. Sci. Technol.*, vol. 26, no. 1, pp. 81–92, 2012, doi: 10.1007/s12206-011-1014-7.